Identification of novel genes associated with fracture healing in osteoporosis induced by Krm2 overexpression or Lrp5 deficiency

FENG GAO[1], FENG XU[2], DANKAI WU[1], JIEPING CHENG[1] and PENG XIA[1]

[1]Department of Orthopedics, The Second Hospital of Jilin University, Changchun, Jilin 130041;
[2]Department of Spine Surgery, The First Hospital of Jilin University, Changchun, Jilin 130021, P.R. China

Received January 20, 2016; Accepted January 30, 2017

DOI: 10.3892/mmr.2017.6544

Abstract. The aim of the present study was to screen potential key genes associated with osteoporotic fracture healing. The microarray data from the Gene Expression Omnibus database accession number GSE51686, were downloaded and used to identify differentially expressed genes (DEGs) in fracture callus tissue samples obtained from the femora of type I collagen (*Col1a1)*-kringle containing transmembrane protein 2 (*Krm2)* mice and low density lipoprotein receptor-related protein $5^{-/-}$ ($Lrp5^{-/-}$) transgenic mice of osteoporosis compared with those in wild-type (WT) mice. Enrichment analysis was performed to reveal the DEG function. In addition, protein-protein interactions (PPIs) of DEGs were analyzed using the Search Tool for the Retrieval of Interacting Genes database. The coexpression associations between hub genes in the PPI network were investigated, and a coexpression network was constructed. A total of 841 DEGs (335 upregulated and 506 downregulated) were identified in the *Col1a1-Krm2* vs. the WT group, and 50 DEGs (16 upregulated and 34 downregulated) were identified in the $Lrp5^{-/-}$ vs. the WT group. The DEGs in *Col1a1-Krm2* mice were primarily associated with immunity and cell adhesion (GO: 0007155) functions. By contrast, the DEGs in $Lrp5^{-/-}$ mice were significantly associated with muscle system process (GO: 0003012) and regulation of transcription (GO: 0006355). In addition, a series of DEGs demonstrated a higher score in the PPI network, and were observed to be coexpressed in the coexpression network, and included thrombospondin 2 (*Thbs2*), syndecan 2 (*Sdc2*), FK506 binding protein 10 (*Fkbp10*), 2'-5'-oligoadneylate synthase-like protein 2 (*Oasl2)*, interferon induced protein with tetratricopeptide repeats (*Ifit*) 1 and *Ifit2*. *Thbs2* and *Sdc2* were significantly correlated with extracellular matrix-receptor interactions. The results suggest that *Thbs2*, *Sdc2*, *Fkbp10*, *Oasl2*, *Ifit1* and *Ifit2* may serve important roles during the fracture healing process in osteoporosis. In addition, this is the first study to demonstrate that *Sdc2*, *Fkbp10*, *Oasl2*, *Ifit1* and *Ifit2* may be associated with osteoporotic fracture healing.

Correspondence to: Dr Feng Xu, Department of Spine Surgery, The First Hospital of Jilin University, 71 Xinmin Street, Chaoyang, Changchun, Jilin 130021, P.R. China
E-mail: xufengtx1978@163.com

Dr Dankai Wu, Department of Orthopedics, The Second Hospital of Jilin University, 218 Zi Qiang Street, Changchun, Jilin 130041, P.R. China
E-mail: wudankai@163.com

Abbreviations: DEGs, differentially expressed genes; PPIs, protein-protein interactions; BMP-2, bone morphogenetic protein-2; PTH, parathyroid hormone; *LRP5,* lipoprotein receptor-related protein 5; *KREMEN2,* kringle containing transmembrane protein 2; DKK1, dickkopf homolog 1; GEO, Gene Expression Omnibus database; RMA, robust microarray analysis; FDR, false discovery rate; GO, Gene Ontology; KEGG, Kyoto Encyclopedia of Genes and Genomes; DAVID, Database for Annotation, Visualization and Integrated Discovery; STRING, Search Tool for the Retrieval of Interacting Genes; PCC, pearson correlation coefficient; CAMs, cell adhesion molecules; *Thbs2,* thrombospondin 2; *Sdc2,* syndecan 2; *Fkbp10,* FK506 Binding Protein 10

Key words: fracture healing, osteoporosis, gene, network, coexpression

Introduction

Osteoporotic fracture is a common event in the elderly, resulting in substantial mortality, and the mortality rate of hip fracture for 6 months is ~10-20% (1). The prevalence of osteoporotic fractures, hip fractures in particular, is increasing in many regions of the world (2). Current therapies focus on the prevention and treatment of osteoporotic fractures; however, this may easily lead to complications, thus it remains a worldwide public health concern. Therefore, a greater understanding of the underlying molecular mechanisms of fracture healing in the osteoporotic bone is required, as well as identifying candidate biomarkers for osteoporotic fracture therapies.

Over the past few years, a number of remarkable achievements have been made in the genetic study of fracture healing in osteoporosis. One such study demonstrated that transgenesis of bone morphogenetic protein-2 promotes fracture healing in osteoporosis by inducing increased callus density and a larger cross-sectional callus area (3). During remodeling of fractured bone, parathyroid hormone (PTH) promotes the formation of osteoclasts

to restore the mechanical strength and structure of bones, and polymorphisms in genes encoding PTH influence the genetic regulation of bone mineral density (4). Low density lipoprotein receptor-related protein 5 (*LRP5*) serves a significant functional role in skeletal homeostasis, and mutations in *LRP5* induce a variety of bone density-associated diseases (5). *Lrp5* deficiency results in decreased osteoblast proliferation and function, which induces a low bone mass phenotype (6). Kringle containing transmembrane protein 2 (*KREMEN2*), also known as *KRM2*, is a high-affinity transmembrane receptor of dickkopf homolog 1, and is thought to be a regulator of bone remodeling (7). It has been demonstrated that *Krm2*$^{-/-}$ mice develop a high bone mass phenotype and overexpression of *Krm2* in type I collagen (*Col1a1)-Krm2* transgenic mice induces severe osteoporosis with decreased levels of osteoblasts and elevated osteoclast differentiation (8). Using a model of fracture healing in *Col1a1-Krm2* transgenic mice and *Lrp5*$^{-/-}$ mice, a previous study revealed that fracture healing is greatly damaged in *Col1a1-Krm2* transgenic mice and *Lrp5*$^{-/-}$ mice; however, the *Col1a1-Krm2* mice were more severely impaired than *Lrp5*$^{-/-}$ mice (9). In addition, this previous study identified a set of differentially expressed genes (DEGs) in the two mouse models using microarray analysis (9). However, DEG interactions and functions require further investigation in order to provide a more comprehensive understanding of the effect of osteoporosis on fracture healing.

In order to investigate the interactions and functions of DEGs in *Col1a1-Krm2* transgenic mice and *Lrp5*$^{-/-}$ mice further, the microarray data obtained by Liedert *et al* (9) were analyzed in the present study. Following identification of DEGs, enrichment analysis was performed. In addition, protein-protein interactions (PPIs) of DEGs and hub genes in the PPI network were analyzed. Furthermore, coexpression associations between hub genes and additional DEGs were examined. These results may contribute to a greater understanding of the effect of osteoporosis on fracture healing, and provide novel information that facilitates the development of future clinical therapies for osteoporotic fractures.

Materials and methods

Affymetrix microarray data. The raw gene expression profile dataset GSE51686 (9) was obtained from the Gene Expression Omnibus (GEO) database (http://www.ncbi.nlm.nih.gov/geo/). The data was generated by the (Mouse430_2) Affymetrix Mouse Genome 430 2.0 Array platform (GEO accession, GPL1261; Affymetrix, Inc., Santa Clara, CA, USA). This dataset contained 9 fracture callus tissue samples obtained from the femora at 10 days following osteotomy in the wild-type (WT) mice (n=3), *Col1a1-Krm2* transgenic mice with severe osteoporosis (n=3), and *Lrp5*$^{-/-}$ mice with low bone mass (n=3), respectively. All mice were female and 26 weeks of age.

The CEL and probe annotation files for this dataset were downloaded. The raw expression data were preprocessed by background correction, quantile normalization and probe summarization using the robust microarray analysis algorithm in the affy package (version 3.3.2) (10) of Bioconductor (version 3.4; http://www.bioconductor.org/). Subsequently, the org.Hs.eg.db (version 3.4.0) (11) and illuminaHumanv3.db (version 1.26.0) (12) packages of Bioconductor were used to translate probe identifications (IDs) to gene symbols. If one gene symbol was matched by multiple probe IDs, the mean expression value was selected as the expression level of this gene.

Identification of DEGs. DEGs in *Col1a1-Krm2* mice and *Lrp5*$^{-/-}$ mice compared with the WT controls were identified using the linear models for microarray data (LIMMA) package (version 3.30.3; http://www.bioconductor.org/packages/release/bioc/html/limma.html) (13), which is a commonly used tool for the identification of DEGs. The P-value for each gene was calculated using the unpaired t-test in LIMMA, which was then adjusted for the false discovery rate (FDR) using the Benjamini-Hochberg method (14). Only the genes with FDR values <0.05 and $\log_2$ fold change values ≥ 0.5 were selected as DEGs.

The Venny online tool (version 2.0; http://bioinfogp.cnb.csic.es/tools/venny/index.html) (15) was utilized to construct Venn diagrams for the upregulated and downregulated genes identified between the *Col1a1-Krm2* vs. WT and *Lrp5*$^{-/-}$ vs. WT groups.

Enrichment analysis of DEGs. Functional Gene Ontology (GO) and Kyoto Encyclopedia of Genes and Genomes (KEGG) pathway enrichment analyses of upregulated and downregulated genes were performed using the Database for Annotation Visualization and Integrated Discovery (version 6.8; http://david.abcc.ncifcrf.gov/) database (16). The P-value was calculated using the modified Fisher's exact test, and $P<0.05$ was considered to indicate a statistically significant difference. A gene count in each term ≥ 2 was set as the cut-off criteria. Additional parameters were set to the default values.

Construction of PPI networks. PPIs of DEGs were obtained from the Search Tool for the Retrieval of Interacting Genes database (version 10.0; http://string-db.org/), which integrates a variety of known and predicted protein associations (17). The combined score for each PPI was calculated, and a score of >0.4 was set as the cut-off criterion. Additional parameters were set to the default values. The PPI network was visualized using the Cytoscape software (version 3.4.0; http://cytoscape.org/), which is an open access software for visualizing biomolecular networks (18). In the network, 'node' represents a gene or protein, and 'line' represents an interaction between the two nodes. The degree of each node (number of interactions with other proteins) is equal to the number of nodes that interacted with this node.

Analysis of hub genes in the PPI network. Hub genes refer to the relatively key genes in the network. Hub genes were identified using three centricity methods in the PPI network, including the degree centrality (19), betweenness centrality (20) and subgraph centrality methods (21). The scores obtained from the degree, betweenness and subgraph methods were calculated using the CytoNCA plug-in (version 2.1.6) (22) in Cytoscape. High scores for the degree, betweenness and subgraph methods indicated that the nodes

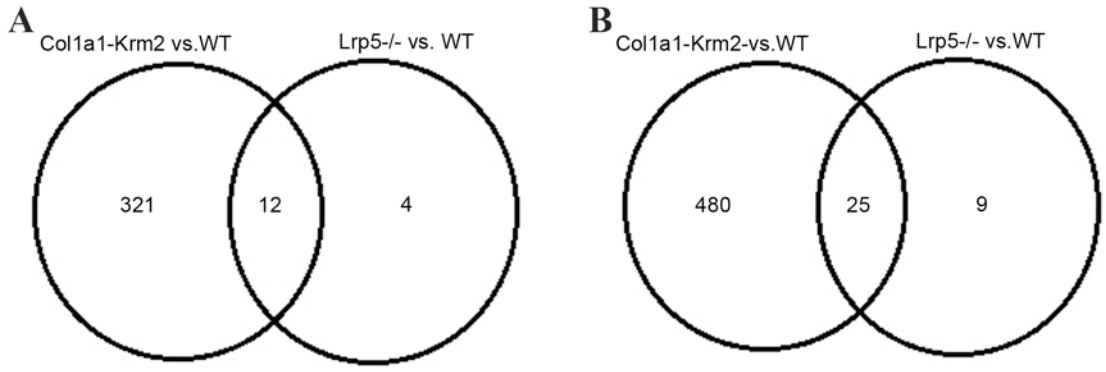

Figure 1. Venn diagrams of differentially expressed genes between *Col1a1-Krm2* vs. WT and *Lrp5*$^{-/-}$ vs. WT groups. (A) Venn diagram of upregulated genes. (B) Venn diagram of downregulated genes. *Col1a1*, type I collagen; *Krm2*, kringle containing transmembrane protein 2; *Lrp5*, low density lipoprotein receptor-related protein 5; *Col1a1-Krm2*, *Col1a1-Krm2* transgenic mice; *Lrp5*$^{-/-}$, mice deficient in *Lrp5*; WT, wild-type mice.

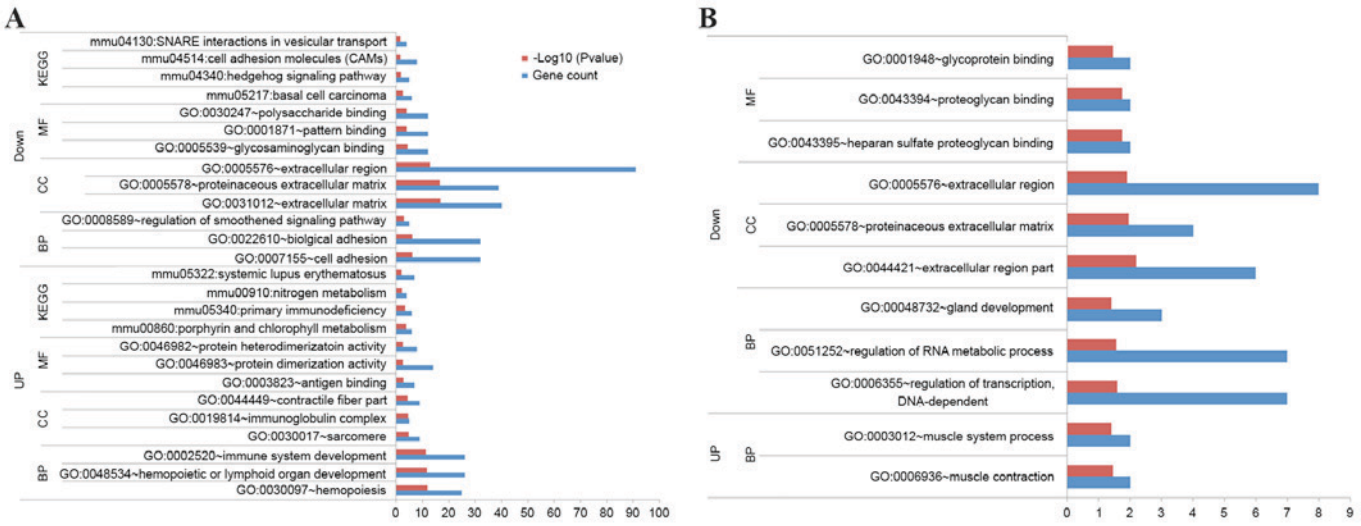

Figure 2. GO and KEGG pathway terms enriched by differentially expressed genes between (A) *Col1a1-Krm2* transgenic mice and wild-type mice and (B) *Lrp5*$^{-/-}$ mice and wild-type mice. 'Up' represents upregulated genes and 'Down' represents downregulated genes. Red bars indicate the P-values, and blue bars indicate the gene count. GO, Gene Ontology; KEGG, Kyoto Encyclopedia of Genes and Genomes; *Col1a1*, type I collagen; *Krm2*, kringle containing transmembrane protein 2; *Lrp5*, low density lipoprotein receptor-related protein 5; BP, biological process; CC, cellular component; MF, molecular function.

were more significant in the network. Hierarchical clustering of hub genes with higher scores was performed using the pvclust R package (version 1.3-2) (23).

Coexpression associations of hub genes with DEGs. The Pearson's correlation coefficient (PCC) method (24) was used to identify the coexpression associations of hub genes with other DEGs. Only coexpression associations with PCC values of >0.9 were selected for analysis. A PCC value of >0 indicated that the two genes were positively correlated, and a PCC value of <0 indicated that the two genes were negatively correlated.

Results

Statistical analysis. Based on the cut-off criteria, a total of 841 DEGs (335 upregulated and 506 downregulated) and 50 DEGs (16 upregulated and 34 downregulated) were identified in the *Col1a1-Krm2* and *Lrp5*$^{-/-}$ mice when compared with WT mice, respectively. When compared with WT mice, 12 of these genes were upregulated and 25 were downregulated in the *Col1a1-Krm2* and *Lrp5*$^{-/-}$ mice (Fig. 1).

DEG function. To further reveal gene function in the two groups, GO and KEGG pathway enrichment analyses were performed. In the *Col1a1-Krm2* vs. WT group, the upregulated genes were primarily associated with hemopoiesis (GO: 0030097), hemopoietic or lymphoid organ (GO: 0048534) and immune system development (GO: 0002520), as well as pathways associated with primary immunodeficiency (mmu05340) and nitrogen metabolism (mmu00910) (Fig. 2A). The downregulated genes were significantly associated with cell adhesion (GO: 0007155) and regulation of the smoothened signaling pathway, as well as the hedgehog signaling pathway (mmu04340) and cell adhesion molecules (mmu04514) (Fig. 2A).

In the *Lrp5*$^{-/-}$ vs. WT group, the upregulated genes were implicated in muscle contraction (GO: 0006936) and muscle system process (GO: 0003012) (Fig. 2B). The downregulated genes were markedly associated with the regulation of

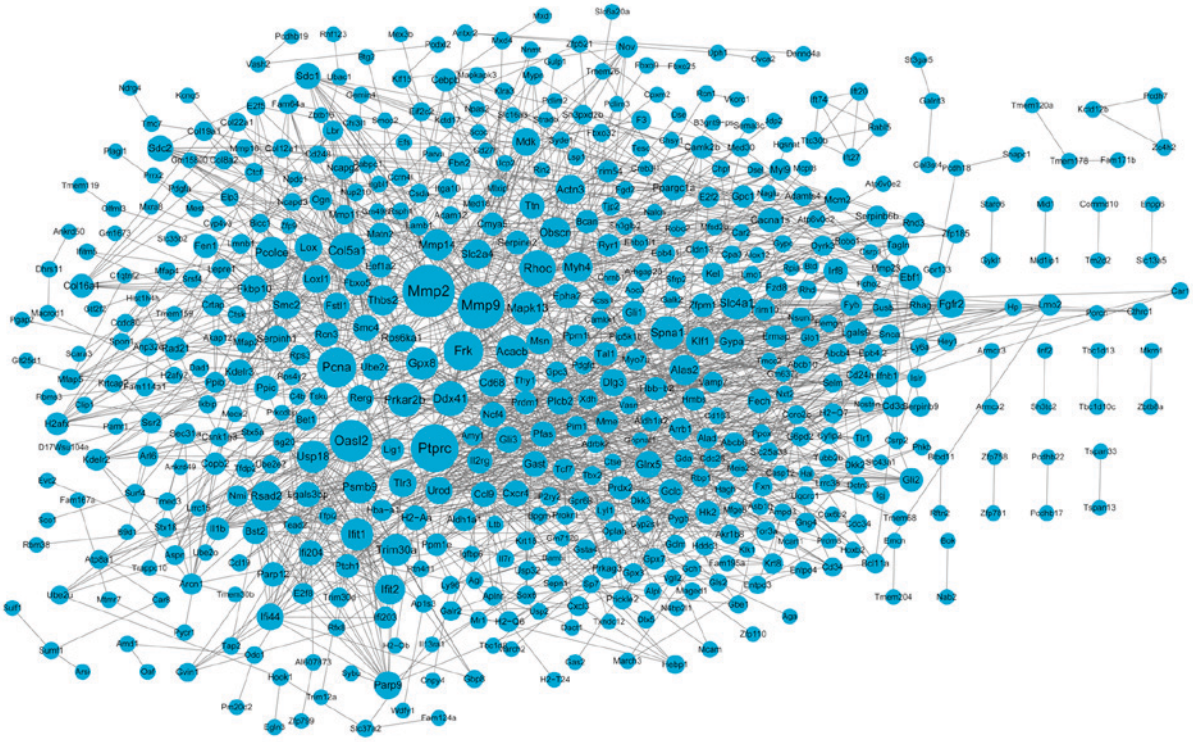

Figure 3. Protein-protein interaction network of differentially expressed genes as determined using the Search Tool for the Retrieval of Interacting Genes database (http://string-db.org/). Each node represents a protein, and each line represents the interaction between the two proteins.

transcription (GO: 0006355) and RNA metabolic processes (GO: 0051252) (Fig. 2B). No significant pathways were enriched by the upregulated genes.

Analysis of PPI network. In order to determine interactions between DEGs, a PPI network was constructed. The network was composed of 551 nodes and 1,608 PPIs (Fig. 3). Based on the centricity methods, the top 40 nodes with the highest scores in the PPI network were selected as hub genes for further analysis, including 2'-5'-oligoadneylate synthase-like protein 2 (*Oasl2*), thrombospondin 2 (*Thbs2*), syndecan 2 (*Sdc2*), FK506 binding protein 10 (*Fkbp10*), interferon induced protein with tetratricopeptide repeats *(Ifit)* 1 and *Ifit2* (Table I). Following the removal of duplicates in Table I, a total of 66 genes remained, which were clustered into two groups and used to distinguish the WT, *Col1a1-Krm2* and *Lrp5*$^{-/-}$ samples in a heat map (Fig. 4).

The 66 hub genes were significantly associated to the five signaling pathways (Table II). Matrix metalloproteinase (Mmp) 2 and Mmp9 were associated with the leukocyte transendothelial migration pathway, whereas *Thbs2* and *Sdc2* were associated with the extracellular matrix (ECM)-receptor interaction pathway. The protein tyrosine phosphatase receptor type C and *Sdc2* were implicated in the cell adhesion molecule pathway (Table II).

Analysis of the coexpression network. In order to investigate the coexpression associations between the selected hub genes and additional DEGs, a coexpression network was constructed. A total of 21 hub genes were determined to coexpress with additional DEGs (Fig. 5). A set of hub genes were observed to coexpress with each other, including *Thbs2*, *Sdc2* and *Fkbp10*, as well as *Oasl2*, *Ifit1* and *Ifit2* (Fig. 5).

Table I. Top 40 nodes with a high score in the protein-protein interaction network.

A, Subgraph

Node	Score
Mmp2	132118.94
Oasl2	115994.88
Ifit1	95969.49
Trim30a	92368.98
Mmp9	89980.91
Usp18	87137.86
Ifit2	83711.57
Rsad2	78389.78
Parp9	65845.10
Psmb9	62329.73
Ifi44	61890.17
Ptprc	60581.35
Bst2	52788.61
Lgals3bp	52307.49
Parp12	50636.56
Col5a1	42741.73
Ifi204	32780.95
Thbs2	32724.00
Tlr3	32063.93
Lgals9	30456.22
Pcolce	27954.06
Mmp14	27788.79
Ifi203	27352.81
Pcna	26264.86

Table I. Continued.

A, Subgraph

Node	Score
Nmi	25586.03
Frk	25365.84
Loxl1	24301.15
Lox	23572.33
Isg20	21952.91
Rhoc	20744.50
Mdk	20643.03
Fstl1	20386.14
Ddx41	19990.48
Sdc1	18627.42
Serpinh1	17851.99
Gpx8	17771.15
Rcn3	17400.74
Cd68	17032.79
Sdc2	14213.72
Fkbp10	14067.95

B, Degree

Mmp2	47.00
Ptprc	41.00
Mmp9	40.00
Oasl2	34.00
Pcna	31.00
Frk	31.00
Col5a1	27.00
Rhoc	27.00
Ddx41	25.00
Prkar2b	24.00
Spna1	23.00
Mapk13	23.00
Ifit1	22.00
Usp18	22.00
Psmb9	22.00
Gpx8	22.00
Acacb	22.00
Slc4a1	22.00
Trim30a	21.00
Pcolce	21.00
Mmp14	20.00
Obscn	20.00
Ifit2	19.00
Rsad2	19.00
Thbs2	19.00
Myh4	19.00
Alas2	19.00
Slc2a4	18.00
Actn3	18.00
Klf1	17.00
Parp9	16.00
Tlr3	16.00

Table I. Continued.

B, Degree

Node	Score
Loxl1	16.00
Lox	16.00
Mdk	16.00
Fgfr2	16.00
Smc2	16.00
Ifi44	15.00
Cd68	15.00
Fkbp10	15.00

C, Betweenness

Ptprc	30306.94
Mmp2	30018.82
Pcna	26498.73
Oasl2	24770.62
Frk	20782.62
Rhoc	17367.36
Acacb	16584.40
Mmp9	16291.33
Spna1	13323.41
Mapk13	13268.12
Prkar2b	11615.84
Gpx8	11494.19
Slc2a4	11248.73
Ddx41	10606.64
Obscn	10462.83
Pfas	9557.37
Psmb9	9042.65
Col5a1	8806.07
Rps6ka1	8625.42
Pcolce	7343.19
Mmp14	6612.19
Actn3	6597.27
Dlg3	6507.87
Msn	6370.79
Myh4	6325.04
Alas2	6084.76
Fgfr2	5320.19
Glrx5	5243.41
Mdk	5180.35
Slc4a1	5082.71
Atp8a1	5063.36
Copb2	5019.16
Ppargc1a	4905.46
Cd68	4728.94
H2-Aa	4708.25
Cxcr4	4565.29
Ncf4	4559.99
Rps3	4274.92
Hk2	4171.70
Thbs2	3997.35

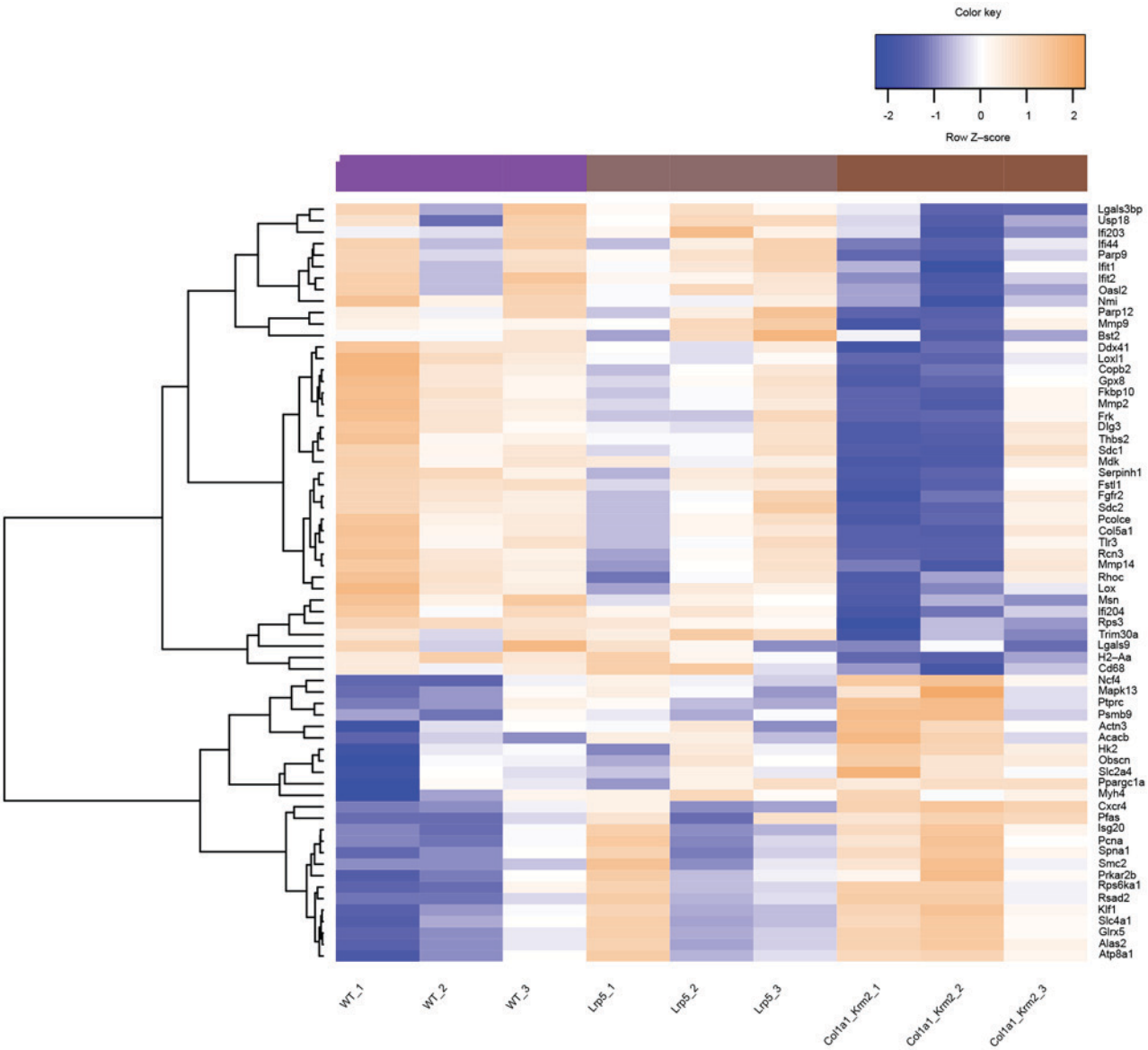

Figure 4. Heat map of hub genes in the protein-protein interaction network in WT, *Lrp5*$^{-/-}$ and *Col1a1-Krm2* mice. Each row represents a single gene and each column represents a sample. The gradual color alteration from orange to blue represents the process from upregulation to downregulation of genes. WT, wild-type; *Col1a1,* type I collagen; *Krm2,* kringle containing transmembrane protein 2; *Lrp5,* low density lipoprotein receptor-related protein 5.

Discussion

In the present study, a set of 841 DEGs (335 upregulated and 506 downregulated) and 50 DEGs (16 upregulated and 34 downregulated) were identified in the *Col1a1-Krm2* vs. WT and *Lrp5*$^{-/-}$ vs. WT groups, respectively. A number of DEGs demonstrated a high score in the PPI network, and were coexpressed in the coexpression network. These genes included *Thbs2*, *Sdc2* and *Fkbp10*, as well as *Oasl2*, *Ifit1* and *Ifit2*. *Thbs2* and *Sdc2* were associated with the ECM-receptor interaction pathway.

Thbs2 is a part of the thrombospondin family and mediates cell-to-cell and cell-to-matrix interactions (25). A previous review reported that disrupted *Thbs2* expression increases cortical bone density, accelerates fracture healing, induces resistance to ovariectomy-induced bone loss and alters the pattern of load-induced bone formation (26). In *Thbs2*-null mice, marrow-derived osteoprogenitor cells are increased, and endosteal bone formation is promoted, indicating that *Thbs2* modulates the proliferation of osteoprogenitor cells and bone remodeling (27,28). *Sdc2* functions as an integral membrane protein and mediates cell-to-matrix interactions via its ECM protein receptor (29). *Sdc2* is a crucial determinant of chemosensitivity in osteoblasts, and it stimulates the mitogenic activity of granulocyte-macrophage colony-stimulating factor (30). *Fkbp10* is a part of the FKBP-type peptidyl-prolyl cis/trans isomerase family and interacts with collagens (31). A homozygous splicing mutation in *Fkbp10* leads to osteogenesis imperfecta with a mineralization defect via a reduction in bone collagen content (32,33). There is no direct evidence to implicate *Sdc2* and *Fkbp10* in osteoporotic fracture healing, however, they are thought to coexpress with *Thbs2*. Therefore, *Sdc2* and *Fkbp10*, as well as *Thbs2* may serve key roles during the fracture healing process in osteoporosis, via their coexpression associations with each other.

Table II. Pathways enriched by the hub genes in the protein-protein interaction network.

KEGG entry term: pathway	P-value	Gene count	Genes
mmu04670: Leukocyte transendothelial migration	1.82×10^{-5}	7	Mapk13, Cxcr4, Mmp9, Ncf4, Msn, Actn3, Mmp2
mmu04910: Insulin signaling pathway	0.00420	5	Prkar2B, Slc2A4, Hk2, Acacb, Ppargc1A
mmu04512: ECM-receptor interaction	0.00740	4	Sdc1, Thbs2, Col5A1, Sdc2
mmu04514: Cell adhesion molecules	0.03803	4	Ptprc, Sdc1, H2-Aa, Sdc2
mmu04920: Adipocytokine signaling pathway	0.04178	3	Slc2A4, Acacb, Ppargc1A

KEGG, Kyoto Encyclopedia of Genes and Genomes; ECM, extracellular matrix.

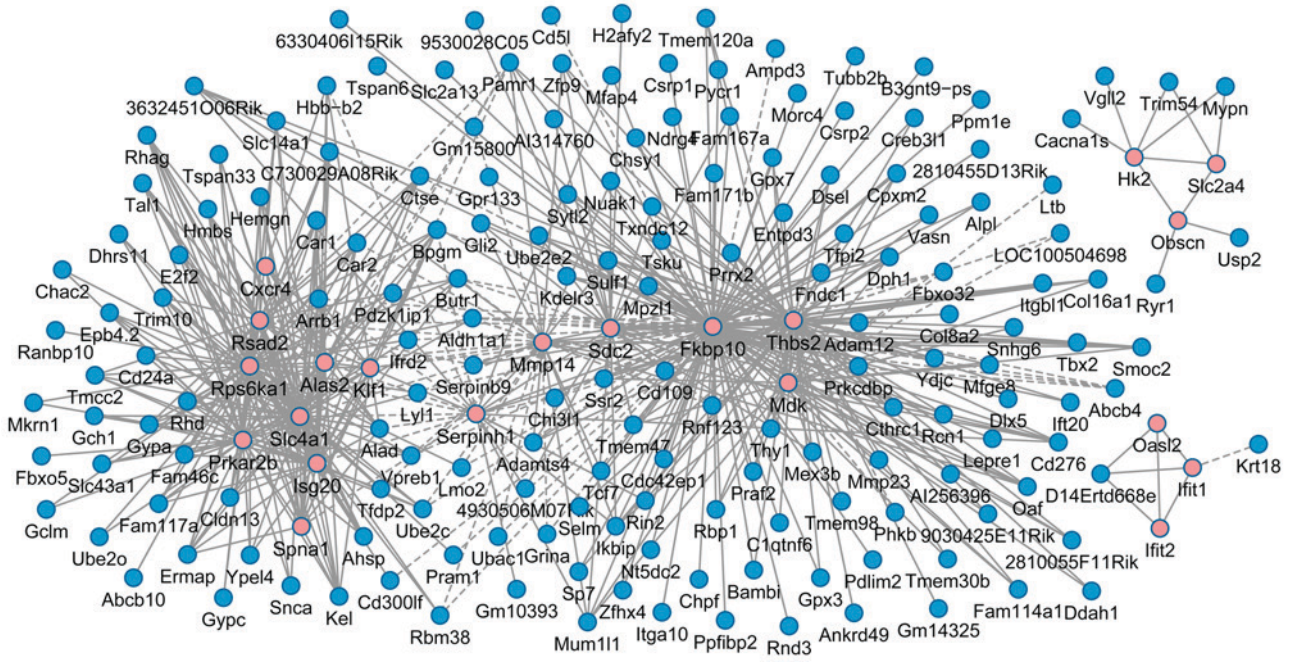

Figure 5. Coexpression network of hub genes and additional differentially expressed genes. Red-colored nodes represent hub genes in the protein-protein interaction network, and blue-colored genes represent differentially expressed genes that are not hub genes. Each node represents a protein, and each line represents the coexpression association between the two genes. Solid lines indicate the coexpression (pearson correlation coefficient) >0.9 (positive correlation), and the dotted lines indicate the coexpression (pearson correlation coefficient) <0.9 (negative correlation).

In the present study, *Oasl2*, *Ifit1* and *Ifit2* demonstrated high scores in the PPI network and coexpressed with each other. *Ifit1* and *Ifit2* were interferon-induced proteins containing tetratricopeptide repeats (34). *Ifit1* is known to be an important innate immune bottleneck (35). During the response of osteoblasts to immune cytokine interferon-β, the expression of *Ifit1* is induced (36). *Ifit2* and *Oasl2* are involved in innate immunity (37,38). Only a limited number of studies have investigated the association between the *Ifit1, Ifit2* and *Oasl2* genes and fracture repair; however they present potential novel candidates for osteoporotic fracture repair therapies.

In the present study, the number of identified DEGs in the *Col1a1-Krm2* vs. WT group was markedly higher than that observed in the *Lrp5*$^{-/-}$ vs. WT group, which was consistent with previous findings (9). According to the DEGs enrichment analysis, the DEGs in the *Col1a1-Krm2* vs. WT group were primarily associated with immunity and cell adhesion. By contrast, the DEGs in the *Lrp5*$^{-/-}$ vs. WT group were significantly associated with muscle system processes (GO: 0003012) and the regulation of transcription (GO: 0006355). These results suggest that during the fracture repair process in osteoporosis, the DEGs induced by *Krm2* overexpression or *Lrp5* deficiency, and their functions, may be distinctly different.

Compared with the findings presented by Liedert *et al* (9), the present study identified the interactions and coexpression patterns among a set of genes, which was not determined previously. However, these predictions require validation in further studies. In a future study, the DEGs and their interactions will be determined in patients.

In conclusion, a series of DEGs, including *Thbs2*, *Sdc2* and *Fkbp10*, as well as *Oasl2*, *Ifit1* and *Ifit2*, demonstrated a significant role in the PPI network and were observed to form co-expression patterns. The results suggest that these genes may serve crucial roles during the fracture repair process in osteoporosis. *Sdc2*, *Fkbp10*, *Oasl2*, *Ifit1* and *Ifit2* were demonstrated to be novel genes associated with osteoporotic fracture healing.

References

1. Namkung-Matthai H, Appleyard R, Jansen J, Hao Lin J, Maastricht S, Swain M, Mason RS, Murrell GA, Diwan AD and Diamond T: Osteoporosis influences the early period of fracture healing in a rat osteoporotic model. Bone 28: 80-86, 2001.
2. Johnell O and Kanis JA: An estimate of the worldwide prevalence and disability associated with osteoporotic fractures. Osteoporos Int 17: 1726-1733, 2006.
3. Egermann M, Baltzer AW, Adamaszek S, Evans C, Robbins P, Schneider E and Lill CA: Direct adenoviral transfer of bone morphogenetic protein-2 cDNA enhances fracture healing in osteoporotic sheep. Hum Gene Ther 17: 507-517, 2006.
4. Noordin S and Glowacki J: Parathyroid hormone and its receptor gene polymorphisms: Implications in osteoporosis and in fracture healing. Rheumatol Int 36: 1-6, 2016.
5. Mizuguchi T, Furuta I, Watanabe Y, Tsukamoto K, Tomita H, Tsujihata M, Ohta T, Kishino T, Matsumoto N, Minakami H, *et al*: LRP5, low-density-lipoprotein-receptor-related protein 5, is a determinant for bone mineral density. J Hum Genet 49: 80-86, 2004.
6. Kato M, Patel MS, Levasseur R, Lobov I, Chang BH, Glass DA II, Hartmann C, Li L, Hwang TH, Brayton CF, *et al*: Cbfa1-independent decrease in osteoblast proliferation, osteopenia, and persistent embryonic eye vascularization in mice deficient in Lrp5, a Wnt coreceptor. J Cell Biol 157: 303-314, 2002.
7. Mao B, Wu W, Davidson G, Marhold J, Li M, Mechler BM, Delius H, Hoppe D, Stannek P, Walter C, *et al*: Kremen proteins are Dickkopf receptors that regulate Wnt/beta-catenin signalling. Nature 417: 664-667, 2002.
8. Schulze J, Seitz S, Saito H, Schneebauer M, Marshall RP, Baranowsky A, Busse B, Schilling AF, Friedrich FW, Albers J, *et al*: Negative regulation of bone formation by the transmembrane Wnt antagonist Kremen-2. PLoS One 5: e10309, 2010.
9. Liedert A, Röntgen V, Schinke T, Benisch P, Ebert R, Jakob F, Klein-Hitpass L, Lennerz JK, Amling M and Ignatius A: Osteoblast-specific Krm2 overexpression and Lrp5 deficiency have different effects on fracture healing in mice. PLoS One 9: e103250, 2014.
10. Gautier L, Cope L, Bolstad BM and Irizarry RA: affy-analysis of Affymetrix GeneChip data at the probe level. Bioinformatics 20: 307-315, 2004.
11. Carlson M: org.Hs.eg.db: Genome wide annotation for Human. R package version 3.4.0, 2015.
12. Dunning M, Lynch A and Eldridge M: illuminaHumanv3.db: Illumina HumanHT12v3 annotation data (chip illuminaHumanv3). R package version 1.26.0, 2015.
13. Ritchie ME, Phipson B, Wu D, Hu Y, Law CW, Shi W and Smyth GK: limma powers differential expression analyses for RNA-sequencing and microarray studies. Nucleic Acids Res 43: e47, 2015.
14. Glueck DH, Mandel J, Karimpour-Fard A, Hunter L and Muller KE: Exact calculations of average power for the Benjamini-Hochberg procedure. Int J Biostat 4: Article 11, 2008.
15. Oliveros JC: VENNY. An interactive tool for comparing lists with Venn Diagrams. 2007. http://bioinfogp.cnb.csic.es/tools/venny/index.html. Accessed November 20, 2013.
16. Huang DW, Sherman BT, Tan Q, Collins JR, Alvord WG, Roayaei J, Stephens R, Baseler MW, Lane HC and Lempicki RA: The DAVID gene functional classification tool: A novel biological module-centric algorithm to functionally analyze large gene lists. Genome Biol 8: R183, 2007.
17. Szklarczyk D, Franceschini A, Wyder S, Forslund K, Heller D, Huerta-Cepas J, Simonovic M, Roth A, Santos A, Tsafou KP, *et al*: STRING v10: Protein-protein interaction networks, integrated over the tree of life. Nucleic Acids Res 43 (Database issue): D447-D452, 2015.
18. Kohl M, Wiese S and Warscheid B: Cytoscape: Software for visualization and analysis of biological networks. Methods Mol Biol 696: 291-303, 2011.
19. Jeong H, Mason SP, Barabási AL and Oltvai ZN: Lethality and centrality in protein networks. Nature 411: 41-42, 2001.
20. Goh KI, Oh E, Kahng B and Kim D: Betweenness centrality correlation in social networks. Phys Rev E Stat Nonlin Soft Matter Phys 67: 017101, 2003.
21. Estrada E and Rodriguez-Velázquez JA: Subgraph centrality in complex networks. Phys Rev E Stat Nonlin Soft Matter Phys 71: 056103, 2005.
22. Tang Y, Li M, Wang J, Pan Y and Wu FX: CytoNCA: A cytoscape plugin for centrality analysis and evaluation of protein interaction networks. Biosystems 127: 67-72, 2015.
23. Suzuki R and Shimodaira H: Pvclust: An R package for assessing the uncertainty in hierarchical clustering. Bioinformatics 22: 1540-1542, 2006.
24. Adler J and Parmryd I: Quantifying colocalization by correlation: The Pearson correlation coefficient is superior to the Mander's overlap coefficient. Cytometry A 77: 733-742, 2010.
25. LaBell TL, Milewicz DJ, Disteche CM and Byers PH: Thrombospondin II: Partial cDNA sequence, chromosome location, and expression of a second member of the thrombospondin gene family in humans. Genomics 12: 421-429, 1992.
26. Alford AI and Hankenson KD: Matricellular proteins: Extracellular modulators of bone development, remodeling, and regeneration. Bone 38: 749-757, 2006.
27. Hankenson KD, Bain SD, Kyriakides TR, Smith EA, Goldstein SA and Bornstein P: Increased marrow-derived osteoprogenitor cells and endosteal bone formation in mice lacking thrombospondin 2. J Bone Miner Res 15: 851-862, 2000.
28. Delany AM and Hankenson KD: Thrombospondin-2 and SPARC/osteonectin are critical regulators of bone remodeling. J Cell Commun Signal 3: 227-238, 2009.
29. Ishikawa-Brush Y, Powell JF, Bolton P, Miller AP, Francis F, Willard HF, Lehrach H and Monaco AP: Autism and multiple exostoses associated with an X;8 translocation occurring within the GRPR gene and 3' to the SDC2 gene. Hum Mol Genet 6: 1241-1250, 1997.
30. Modrowski D, Baslé M, Lomri A and Marie PJ: Syndecan-2 is involved in the mitogenic activity and signaling of granulocyte-macrophage colony-stimulating factor in osteoblasts. J Biol Chem 275: 9178-9185, 2000.
31. Ishikawa Y, Vranka J, Wirz J, Nagata K and Bächinger HP: The rough endoplasmic reticulum-resident FK506-binding protein FKBP65 is a molecular chaperone that interacts with collagens. J Biol Chem 283: 31584-31590, 2008.
32. Venturi G, Monti E, Dalle Carbonare L, Corradi M, Gandini A, Valenti MT, Boner A and Antoniazzi F: A novel splicing mutation in FKBP10 causing osteogenesis imperfecta with a possible mineralization defect. Bone 50: 343-349, 2012.
33. Schwarze U, Cundy T, Pyott SM, Christiansen HE, Hegde MR, Bank RA, Pals G, Ankala A, Conneely K, Seaver L, *et al*: Mutations in FKBP10, which result in Bruck syndrome and recessive forms of osteogenesis imperfecta, inhibit the hydroxylation of telopeptide lysines in bone collagen. Hum Mol Genet 22: 1-17, 2013.
34. Wathelet MG, Clauss IM, Content J and Huez GA: The IFI-56K and IFI-54K interferon-inducible human genes belong to the same gene family. FEBS Lett 231: 164-171, 1988.
35. McDermott JE, Vartanian KB, Mitchell H, Stevens SL, Sanfilippo A and Stenzel-Poore MP: Identification and validation of Ifit1 as an important innate immune bottleneck. PLoS One 7: e36465, 2012.
36. Woeckel VJ, Eijken M, van de Peppel J, Chiba H, van der Eerden BC and van Leeuwen JP: IFNβ impairs extracellular matrix formation leading to inhibition of mineralization by effects in the early stage of human osteoblast differentiation. J Cell Physiol 227: 2668-2676, 2012.
37. Perwitasari O, Cho H, Diamond MS and Gale M Jr: Inhibitor of κB kinase epsilon (IKK(epsilon)), STAT1, and IFIT2 proteins define novel innate immune effector pathway against West Nile virus infection. J Biol Chem 286: 44412-44423, 2011.
38. Zhu J, Ghosh A and Sarkar SN: OASL-a new player in controlling antiviral innate immunity. Curr Opin Virol 12: 15-19, 2015.